Transport and magnetic properties of $YBa_2Cu_3O_{7-\delta}Br_y$ single crystals

P. P. Nguyen, Z. H. Wang, and A. M. Rao
Department of Physics, Massachusetts Institute of Technology, Cambridge, Massachusetts 02139

M. S. Dresselhaus
Department of Physics and Department of Electrical Engineering and Computer Science, Massachusetts Institute of Technology, Cambridge, Massachusetts 02139

J. S. Moodera and G. Dresselhaus
Francis Bitter National Magnet Laboratory, Massachusetts Institute of Technology, Cambridge, Massachusetts 02139

H. B. Radousky and R. S. Glass
Lawrence Livermore National Laboratory, Livermore, California 94550

J. Z. Liu
Department of Physics, University of California–Davis, Davis, California 95616
(Received 28 August 1992; revised manuscript received 18 December 1992)

Deoxygenated nonsuperconducting $YBa_2Cu_3O_{6.2}$ (YBCO) single crystals doped with Br are studied. The resulting crystals become superconducting with $T_c \sim 92$ K, $\Delta T_c \sim 1.0$ K as determined by four-point-probe resistivity measurements. The resistivity in our best sample decreases linearly with temperature. The large ratio in the resistivity at 300 K of the brominated to the pristine YBCO single crystals (~35:1) suggests that bromination greatly increases the scattering rate. The upper critical field $H_{c2}(T)$ parallel and perpendicular to the ab plane is determined resistively. $H_{c2}(0)$ and the corresponding coherence lengths $\xi_{ab}(0)$ and $\xi_c(0)$ are estimated. A comparison with the fully oxygenated YBCO single crystals shows that $\xi_{ab}(0)$ remains approximately the same, whereas $\xi_c(0)$ decreases by a factor of ~ 3, suggesting that Br never enters the CuO_2 planes. The pinning energy for vortex motion in the ab plane decreases after bromination and this decrease can be attributed to the increased anisotropy. For vortex motion along the c axis, however, the pinning energy decreases or increases depending on temperature and field. Compared with the fully oxygenated YBCO single crystals, the critical current density is suppressed by bromination and is strongly dependent on the applied magnetic field. The reduced lower critical field H_{c1} in the brominated YBCO single crystals indicates a reduction in the carrier density (by a factor of between 2 and 3), which is consistent with the observed reduction in the plasma frequency.

I. INTRODUCTION

Halogen doping at modest temperatures (260 °C for Br) has been shown to provide an interesting method for restoring superconductivity in partially deoxygenated nonsuperconducting $YBa_2Cu_3O_{6.2}$ (YBCO) crystals.[1–4] Because of the relatively low processing temperature and the stability of the brominated $YBa_2Cu_3O_{6.2}$ compound to high temperatures (~1000 °C, though further loss of oxygen can occur in the brominated samples at elevated temperatures), these halogenated compounds have attracted attention for possible use in connection with hybrid semiconductor-superconductor integrated circuit devices.

The location of Br in the lattice has also been of great interest because it would give clues to the mechanism for the restoration of superconductivity. Previous attempts to locate the bromine position in the lattice have proved inconclusive, the main reason being that the x-ray diffraction pattern broadens significantly when the bromine is present. Radousky *et al.*[3] conclude that this broadening results from the bromine occupying several nonequivalent sites in the lattice. This point of view has recently been strengthened by the results of Amitin *et al.*,[5] who conclude from detailed NMR work on the YBCO-Cl material that the Cl occupies three separate sites in the lattice.

In this paper we study the temperature and magnetic field dependence of the conductivity and magnetic susceptibility of brominated YBCO, and we relate these properties to the fully oxygenated superconducting YBCO both in the normal and superconducting states. Our goal is to gain further understanding through these transport measurements on the role of Br in restoring superconductivity to deoxygenated YBCO. In Sec. II we discuss sample preparation and characterization, and the experimental procedures. In Sec. III the results of zero magnetic field transport measurements are presented, while Sec. IV is devoted to the corresponding resistivity measurements in a magnetic field parallel and perpendicular to the c axis for temperatures close to T_c. From the resistivity data, the upper critical field H_{c2} can be deduced. Knowledge of H_{c2} is important because H_{c2}

0163-1829/93/48(2)/1148(8)/$06.00

is related to the fundamental length scale of the superconductor and hence to the underlying mechanism for the restoration of superconductivity in brominated YBCO.[6] Section V estimates the pinning potentials for vortex motion parallel and perpendicular to the *ab* plane. Section VI presents the results of the measurements of the critical current density $J_c(T, H)$ and the lower critical field. Section VII summarizes the results of the paper.

II. EXPERIMENT

A. Sample preparation and characterization

The starting materials used for these experiments were small nearly rectangular platelets ($\sim 1.2 \times 0.9$ mm^2 $\times 0.05$ mm thick) of $YBa_2Cu_3O_{7-\delta}$ single crystal with $T_c \sim 92$ K and $\Delta T_c \sim 1.0$ K as determined from resistivity measurements. These crystals were deoxygenated by heating at 600 °C for ~12 h and subsequently brominated for 24 h at 260 °C.[3]

Though the lattice constants of the brominated YBCO single crystals studied here were not measured, previous x-ray diffraction data taken on brominated powder showed an orthorhombic structure which is consistent with the result of others,[3,7–10] with the lattice constants $a = 0.38274 \pm 0.0008$ nm, $b = 0.3880 \pm 0.001$ nm, and $c = 1.1636 \pm 0.004$ nm.[3] These measured lattice constants are similar to the results of a joint x-ray and neutron refinement by Williams *et al.*,[9] though slightly less than those reported by Jorgensen *et al.*[10] Although x-ray data were not obtained on the crystals measured here, the brominated crystals from similar runs were found in general to be twinned as they had been prior to bromination.

Auger depth profiling and energy dispersive x-ray analysis confirmed the uniform incorporation of Br in the deoxygenated $YBa_2Cu_3O_{6.2}$ single crystals with a nominal stoichiometry $YBa_2Cu_3O_{6.2}Br_{0.9}$.[11] Previous work on powders and crystals has shown that for crystals with near 100% magnetic shielding fractions, both weight gain and x-ray fluorescence microprobe measurements find the bromine content to be 0.9 (i.e., $YBa_2Cu_3O_{6.2}Br_{0.9}$). The oxygen content is nominal and is based on similar deoxygenation procedures performed on powders. The oxygen content is assumed not to change during the bromination (since the bromination temperature is low compared with the deoxygenation temperature).[3]

The magnetic susceptibility measurements were carried out using a superconducting quantum interference device (SQUID) to characterize the samples for their shielding fractions. The zero-field-cooled (ZFC) data of Fig. 1, taken with an applied field of 20 Oe parallel to the *c* axis (before demagnetization correction), showed $T_c \simeq 85$ K and $\Delta T_c \simeq 4$ K with a shielding fraction $\simeq 100\%$ for the YBCO, and $T_c \simeq 82$ K and $\Delta T_c \simeq 20$ K with a shielding fraction $\simeq 97\%$ for the brominated YBCO single crystals. (We define T_c by magnetization measurements to be the temperature where the slope of the susceptibility vs T curve is a maximum and calculate ΔT_c from the 10% and 90% points.) These values are to be compared with the zero-field resistivity measurements (described below) of $T_c \simeq 92$ K, $\Delta T_c \simeq 1$ K for both brominated and fully oxygenated YBCO single crystals.

The field-cooled (FC) temperature-dependent susceptibility data showed a small positive increase for both the YBCO and brominated YBCO samples (see Fig. 1). This type of effect has been observed previously[12] and is believed to come from the flux trapping capabilities of the materials and the nonuniform distribution of the magnetic field inside the SQUID.[13]

It is appropriate at this time to mention the question of sample quality, which we believe has caused some confusion over the disparate results in the literature. Since the magnetically determined T_c for the Br-doped sample is lower than that for the pristine one, even though their transport T_c values are about the same, the Br-doped sample is probably more inhomogeneous and impure. Results concluding that the bromine is incorporated in the lattice,[3,5,14] and results indicating that the bromine (or chlorine) causes a decomposition of some parts of the

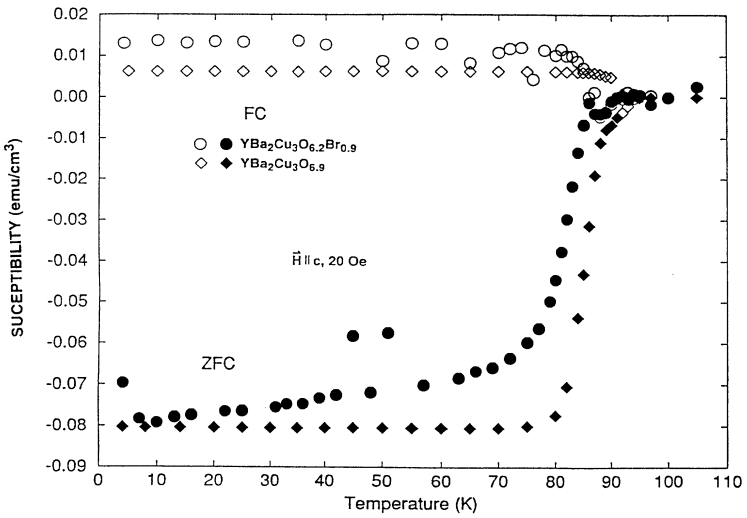

FIG. 1. Susceptibility vs T as determined from SQUID measurements for a fully oxygenated $YBa_2Cu_3O_{6.9}$ single-crystal sample ($T_c = 85$ K) and for a 24-h brominated $YBa_2Cu_3O_{6.2}$ single-crystal sample with a nominal stoichiometry $YBa_2Cu_3O_{6.2}Br_{0.9}$ (Ref. 11) and $T_c = 82$ K. The applied magnetic field is along the *c* axis and has a magnitude of 20 Oe. Both field-cooled (FC) and zero-field-cooled (ZFC) data are shown.

sample, and a reoxygenation of other parts,[15] can both be found. It has been our experience that both types of reactions can occur, without yet determining which uncontrolled factors (e.g., bromine pressure, moisture, initial oxygen content, and ordering, etc.) control the quality of the sample. The samples used here and in our previous studies[6,11] had shielding fractions near 100% and uniform bromine distribution as measured by Auger depth profiling, indicating that the bromine has been incorporated into the lattice. It appears that some of the samples reported in the literature actually did show a decomposition but this is clearly accompanied by shielding fractions that are far below 100%. We believe that the problem of understanding the kinetics of the bromination process is a separate issue from determining the position of the bromine (to be addressed in this paper) which has been demonstrably incorporated into the lattice.

B. Measurements

To make the transport measurements the samples were first mounted on mica with GE varnish. To make good electrical contacts, we used an ion milling technique whereby an aluminum mask was employed to expose only those areas where the silver contact pads were evaporated. Leads were attached using silver paint at the four corners of the sample where contact pads ($\sim$0.1 $\times$ 0.1 mm^2) were deposited. Whereas the contact resistance per pad for the YBCO was only on the order of 0.5 Ω, the contact resistance for the brominated YBCO was $\sim$15 Ω. The contact resistance for both YBCO and brominated YBCO was found to decrease slightly as the temperature decreased from 300 K to 4.2 K.

The resistivity measurements with and without magnetic fields were made using a van der Pauw four-point-probe method. With the magnetic field in the *ab* plane or along the *c* axis, but always perpendicular to most of the current, the magnetoresistance was measured for current flowing in the *ab* plane by sweeping the magnetic field from 0 to 14 T in 20 min. Heating effects were avoided by operating at low current densities ($J \ll J_c$ where J_c is the critical current density). The resistivity measurements were checked for heating effects by increasing the current by a factor of 5–10 and observing no change in the measured ρ_{ab}. The reversibility of the ρ_{ab} versus H measurements was checked by sweeping the field both up and down.

The inductive critical current density of brominated YBCO was obtained by sweeping the applied field between -6 and 6 T at a fixed temperature and using the Bean critical state model formula for $H \parallel c$ axis[16,17]

$$J_c = 30[M_+ - M_-]/D, \tag{1}$$

where M_+ (M_-) is the measured magnetization for increasing (decreasing) field and D is the diameter of the in-plane surface of the sample. For $H \perp c$ axis, a slightly modified formula is used:[17]

$$J_c = 20[M_+ - M_-]/d, \tag{2}$$

where d is the sample thickness.

The lower critical field H_{c1} is defined to be the field

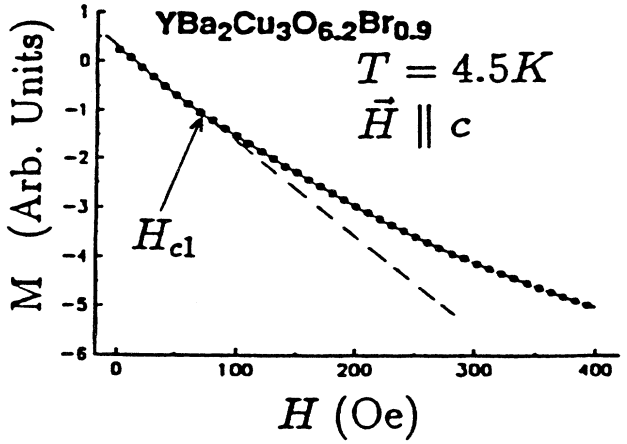

FIG. 2. Magnetization of a $YBa_2Cu_3O_{6.2}Br_{0.9}$ single crystal as a function of field (before demagnetization corrections are applied) at 4.5 K for field perpendicular to the CuO_2 plane. The magnetic field at which the magnetization starts to deviate from the straight line is taken as the criterion for calculating H_{c1}. After demagnetization corrections are applied the field value H_{c1} is about ten times that indicated by the arrow in the figure.

(after applying the sample demagnetization correction) where the magnetization versus field curve starts to deviate from linearity. Figure 2 illustrates the criterion for determining H_{c1}. Using this criterion, H_{c1} versus T was determined.

III. ZERO-FIELD TRANSPORT

Results for the zero-field temperature-dependent resistivity $\rho(T)$ for the starting $YBa_2Cu_3O_{6.9}$ and $YBa_2Cu_3O_{6.2}Br_{0.9}$ single crystals are shown in Fig. 3. There is good agreement between our YBCO data for ρ vs T and the literature values for YBCO single crystals.[18,19] With the seven or eight available contacts per sample, a set of four good contacts is selected, using the T dependence of the resistivity in the normal state and the sharpness of the superconducting transition as the criteria for

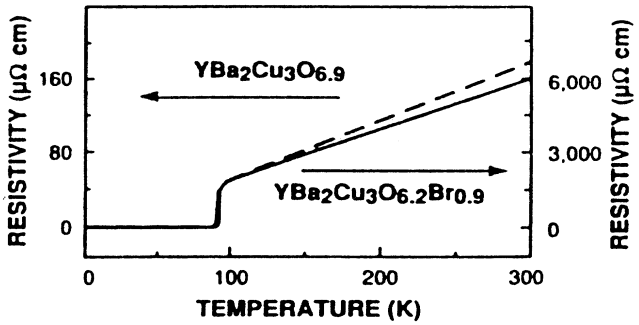

FIG. 3. Measured $\rho(T)$ vs T for a single crystal $YBa_2Cu_3O_{6.2}Br_{0.9}$ ($T_c \simeq$ 92 K) shown by the solid curve. For reference, $\rho(T)$ for a fully oxygenated $YBa_2Cu_3O_{6.9}$ ($T_c \simeq$ 92 K) single crystal is also shown (dashed curve) to illustrate the approximately 35-fold increase in the normal-state resistivity on bromination.

evaluating the quality of the sample and of the contacts. Our best YBCO-Br sample exhibited a zero-field $\rho(T)$ curve similar to that for the $YBa_2Cu_3O_{6.9}$ single crystal used for the starting material, showing a linear T dependence for $\rho(T)$, except that the slope for $\rho(T)$ for the brominated sample (solid curve) is about 35 times larger than that for the starting material (dashed curve). Of the three other YBCO-Br samples, one also showed a linear dependence of $\rho(T)$ with a comparable slope. The remaining two samples which had been subjected to a prolonged acetone and ultrasonic cleaning process exhibited much larger ρ and nonlinear $\rho(T)$ curves.

Despite the large increase in the normal-state resistivity for the brominated samples, they nevertheless demonstrated almost the same T_c values and transition widths (ΔT_c) at the normal-superconducting transition. Note that the two resistivity curves in Fig. 3 almost coalesce if we scale the brominated YBCO curve down by a certain factor ($\simeq 35$) so that the scaled resistivity equals that of the pristine YBCO sample at $\sim$100 K. The room temperature resistivity value for our best brominated YBCO single crystal is accurate only to within 20% due to sample inhomogeneity and slightly nonuniform thicknesses. This value of resistivity for the brominated sample is considerably less than that quoted in Ref. 11 probably because the sample used there had been subjected to a prolonged acetone and ultrasonic cleaning process.

As discussed in Sec. VI, the carrier density in $YBa_2Cu_3O_{6.9}$ single crystals is between two and three times that in $YBa_2Cu_3O_{6.2}Br_{0.9}$. If we assume a Drude expression for the dc resistivity and assume that the effective mass remains the same upon bromination, we can estimate the resistivity for the brominated sample by

$$\frac{\rho_{Br}}{\rho_0} = \frac{n_0\tau_0}{n_{Br}\tau_{Br}} \simeq \frac{2.5\tau_0}{\tau_{Br}}, \tag{3}$$

where ρ_0, n_0, τ_0 and ρ_{Br}, n_{Br}, τ_{Br} are the resistivity, carrier density, and scattering time of the fully oxygenated YBCO and the brominated YBCO single crystals, respectively. Since in this paper we always consider the factor [carrier density/effective mass], the assumption that the effective mass is not changed by bromination can be relaxed by substituting the factor [carrier density/effective mass] for the quantity [carrier density] throughout the text. Experimentally, ρ_{Br}/ρ_0 is approximately 35 at room temperature. This leads us to conclude that bromination greatly increases the scattering rate.

One might argue that the increase of the scattering rate is caused by an increase in the number of impurities and grain boundaries after bromination. Impurities and grain boundaries, however, tend to give rise to only weakly temperature-dependent carrier scattering and hence should have little effect on the temperature dependence (i.e., the slope) of the normal-state resistivity. The 35-fold increase of the slope of the line $\rho(T)$ indicates that impurities and grain boundaries alone cannot account for the remarkable increase of the scattering rate.

IV. UPPER CRITICAL FIELDS

The measured resistivity as a function of magnetic field (both parallel and perpendicular to the c axis) at various temperatures T is shown in Figs. 4 and 5. For each of the lowest temperatures (for either field orientation), the resistivity as a function of field increases from zero with an increasing slope up to some field value above which the slope starts to decrease. The higher-temperature curves seem to follow the same qualitative trend, except that their low-field zero resistivity points are not shown due to a finite remanent value of the applied magnetic field in our superconducting magnet.

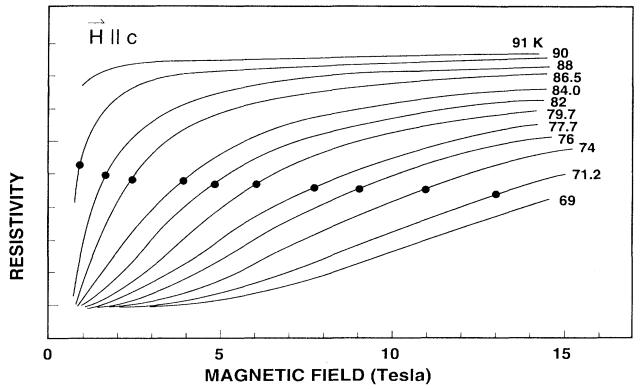

FIG. 4. Magnetic field dependence of the resistivity for $H \parallel c$ axis for a $YBa_2Cu_3O_{6.2}Br_{0.9}$ single crystal as a function of magnetic field for various temperatures from 69 K to 91 K. The 50% points which are taken as the upper critical field are marked with bullets.

Although a sophisticated scaling procedure exists for uniquely determining the upper critical field H_{c2} from the fluctuation conductivity data,[6] the conventional method, in which we define H_{c2} as the field where 50% of the normal-state resistivity is restored, has been shown to give about the same result for $H_{c2}(T)$.[6] Moreover, we are

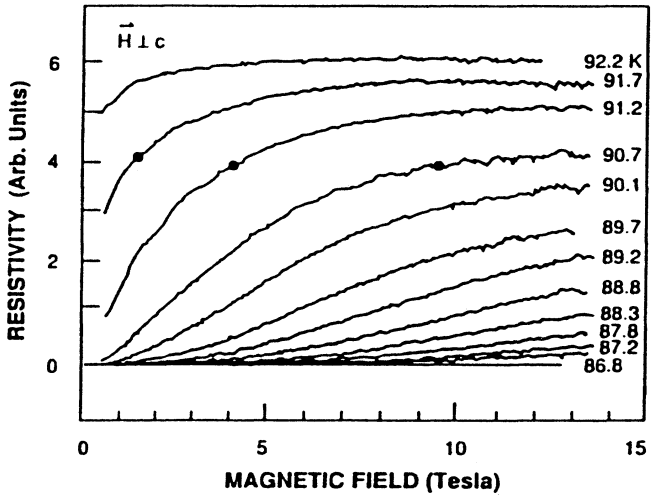

FIG. 5. Magnetic field dependence of the resistivity for $H \perp c$ axis for a single-crystal $YBa_2Cu_3O_{6.2}Br_{0.9}$ sample as a function of magnetic field for various temperatures from 86.8 K to 92.2 K. The 50% points which are taken as the upper critical field are marked with bullets.

mainly interested in the change, not the absolute value, of the magnitude of H_{c2} upon bromination. This change, we believe, can be obtained by consistently applying the same criterion, whether the simple resistive method or the elaborate fluctuation scaling procedure, to both the pristine and the brominated samples. Employing the resistive method, the calculated values for $H_{c2}(T)$ versus T are plotted in Fig. 6 and these results are compared with those from the same batch of $YBa_2Cu_3O_{6.9}$ single crystals before deoxygenation. The results of Fig. 6 show that bromination increases $H_{c2}^{\perp}$ (with $H \perp c$ axis), but decreases $H_{c2}^{\parallel}$ (with $H \parallel c$ axis).

To obtain an estimate for the $T = 0$ values for $H_{c2}(0)$, we use the Werthamer, Helfand, and Hohenberg (WHH) expression[20]

$$H_{c2}(0) = 0.69 \left(\frac{dH_{c2}}{dT} \right) T_c'. \tag{4}$$

Referring to Fig. 6, the slope in Eq. (4) is taken to be tangent to the $H_{c2}(T)$ curve at the highest available field (14 T) for our measurements and T_c' is the intersection of this tangent with the temperature axis. The results for $H_{c2}(0)$ for the brominated and pristine samples are given in Table I for the two magnetic field orientations.

The in-plane and c axis coherence lengths at $T = 0$, $\xi_{ab}(0)$, and $\xi_c(0)$ (Refs. 21 and 22) are estimated from the relations derived from the effective mass model based on the anisotropic Ginzburg-Landau (GL) theory

$$H_{c2}^{\parallel}(0) = \frac{\phi_0}{2\pi\xi_{ab}^2(0)} \tag{5}$$

and

$$H_{c2}^{\perp}(0) = \frac{\phi_0}{2\pi\xi_{ab}(0)\xi_c(0)}, \tag{6}$$

where ϕ_0 is the flux quantum. The results for $\xi_{ab}(0)$ and $\xi_c(0)$ are likewise listed in Table I.

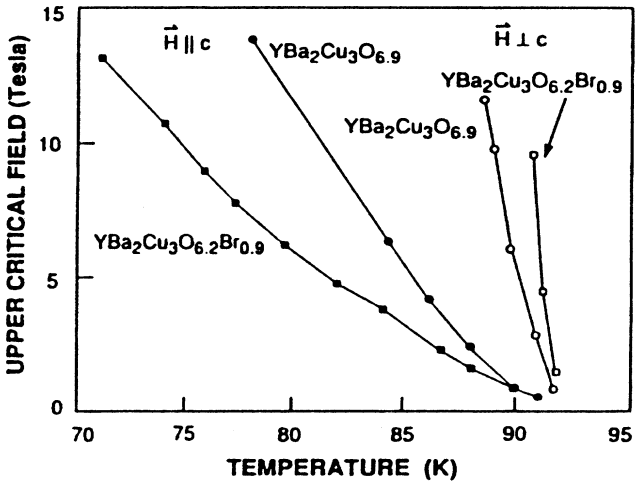

FIG. 6. Upper critical fields $H_{c2}^{\parallel}$ (solid circles and squares) and $H_{c2}^{\perp}$ (open circles and squares) vs T for $YBa_2Cu_3O_{6.9}$ (circles) and $YBa_2Cu_3O_{6.2}Br_{0.9}$ (squares) single crystals.

TABLE I. Parameters deduced from analysis of the critical field measurements.[a]

Parameter	YBCO This work	YBCO Iye[b]	YBCO Moodera[c]	YBCO-Br This work
$H_{c2}^{\parallel}(0)$	78 T	118 T	61 T	53 T
$\xi_{ab}(0)$	21 Å	17 Å	23 Å	25 Å
$H_{c2}^{\perp}(0)$	313 T	510 T	222 T	776 T
$\xi_c(0)$	5.1 Å	3.9 Å	<6.3 Å	1.7 Å

[a] T_c defined at 50% ρ_n.
[b] Reference 21.
[c] Reference 22.

Using the effective mass model, we relate the H_{c2} anisotropy to the effective mass anisotropy by

$$\frac{H_{c2}^{\perp}}{H_{c2}^{\parallel}} = \frac{\xi_{ab}}{\xi_c} = \left(\frac{m_c}{m_{ab}} \right)^{1/2}. \tag{7}$$

Our results from Table I yield a ratio $r = \xi_{ab}(0)/\xi_c(0) \sim 14.6$ and ~ 4.0 for the brominated and pristine YBCO single crystals, respectively. We thus see that bromination has increased the anisotropy of $\xi(0)$ [and $H_{c2}(0)$] by a factor of ~ 3.6. From Eq. (7) we estimate the corresponding changes in the anisotropy of the effective masses upon bromination to be a factor of $\sim$13, as compared with $\sim$4 for the pristine sample.

More specifically, bromination reduces $\xi_c(0)$ by a factor of 3, but leaves $\xi_{ab}(0)$ (or the CuO_2 planes) relatively unaffected. This suggests that Br does not enter the CuO_2 planes. This conclusion is consistent with the findings of Amitin *et al.*[5] that Cl occupies the three positions O(5), O(4), and O(1), all away from the CuO_2 planes.

V. PINNING POTENTIALS

From the data of Figs. 4 and 5, the pinning energy $U(T, B)$ can be obtained using the thermally activated flux motion relation[23,24]

$$U(T, B) = k_B T \ln \left(\frac{\rho_0}{\rho(T)} \right), \tag{8}$$

where ρ_0 is estimated as $\rho_0 = \rho(T_0)$ and T_0 is taken to be the temperature below which the (zero-field) resistivity starts to drop rapidly.[24] The uncertainty in T_0 introduces a small systematic error, but this error does not significantly affect our comparison of $U(T, B)$ between the pristine and brominated YBCO single crystals. Figures 7(a) and 7(b) show such a comparison as a function of field for $H \parallel c$ at $T = 89.2$ K and $H \perp c$ at $T = 76.0$ K, respectively. The horizontal lines correspond to $U \sim k_B T$ and indicate the crossover between the thermally activated dissipation (upper) and the flux flow (lower) regions. Note that no data points are given in the flux flow region since Eq. (8), which describes thermally activated flux motion, no longer applies here. Similarly, Figs. 8(a) and 8(b) compare the pinning energies as a function of temperature at 5 T for both field orientations. Again, flux flow and thermally activated dissipation dominate

the regions below and above the straight lines $U \sim k_B T$, respectively.

From Figs. 7(a) and 8(a), bromination appears to decrease the pinning energy for vortices aligned along the c axis. A possible explanation for the pinning potential reduction is the increase of anisotropy[25] discussed above. Since

$$U = J_c B R_c^2 L_c r_p, \tag{9}$$

where r_p is the range of the pinning potential, R_c is the correlation length of the vortices in the ab plane, and L_c is the correlation length along the vortex, higher anisotropy or shorter correlation length means smaller pinning energy, assuming the other parameters r_p, R_c, and J_c remain the same in the ab plane. (J_c in the ab plane, as shown in Sec. VI, is in fact smaller at high field for the brominated YBCO samples, reducing the pinning potential even further.)

For magnetic fields parallel to the ab plane, the anisotropy argument is inapplicable since the pinning mechanism is different and is believed to arise from the strong modulation of the order parameter in the direction perpendicular to the layers.[26] As a result, the pinning energy for vortex motion perpendicular to the layers does not always increase for the more anisotropic brominated YBCO samples. In fact, as shown in Figs. 7(b) and 8(b), the pinning potential is smaller than that of the fully oxygenated YBCO single crystals at low temperature and field.

VI. MAGNETIZATION MEASUREMENTS

Figures 9 and 10 present the critical current density J_c calculated from the magnetization hysteresis data using the modified Bean critical-state model for magnetic field parallel and perpendicular to the c axis. Compared

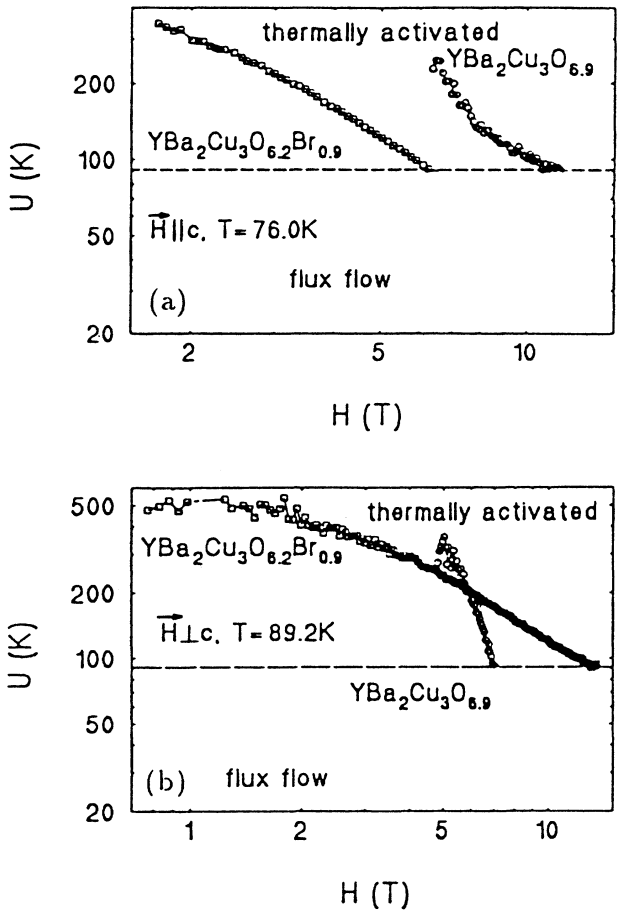

FIG. 7. (a) The field dependence at 76.0 K of the activation energy U for flux motion in the ab plane ($H \parallel c$) derived from the resistivity data for $YBa_2Cu_3O_{6.9}$ (open circles) and $YBa_2Cu_3O_{6.2}Br_{0.9}$ (open squares) single crystals. The horizontal dashed line $U(T) = k_B T$ separates the flux flow from the thermally activated flux motion regions. (b) The corresponding field dependence at 89.2 K of the activation energy for the flux motion perpendicular to the ab plane ($H \perp c$).

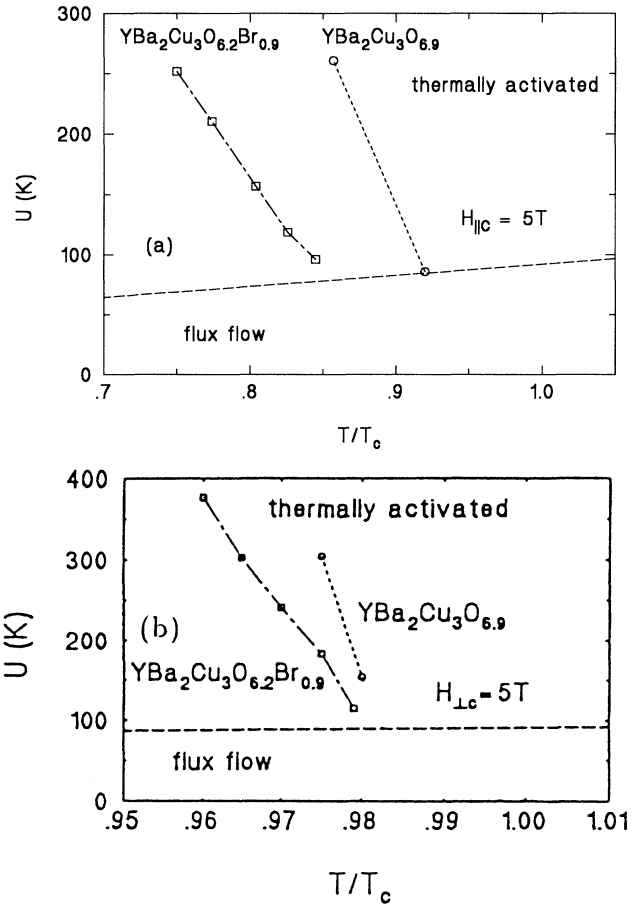

FIG. 8. (a) The temperature dependence at 5 T ($H \parallel c$) of the activation energy for the flux motion in the ab plane derived from the resistivity data for $YBa_2Cu_3O_{6.9}$ (open circles) and $YBa_2Cu_3O_{6.2}Br_{0.9}$ (open squares) single crystals. The dashed line denoting $U(T) = k_B T$ separates the flux flow from the thermally activated flux motion regions. (b) The corresponding temperature dependence at 5 T (for $H \perp c$) of the activation energy for flux motion perpendicular to the ab plane.

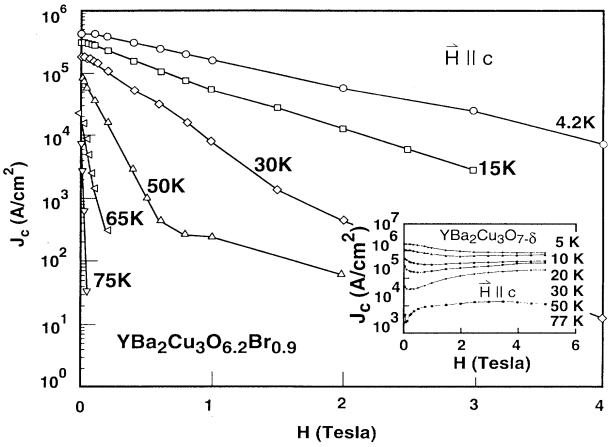

FIG. 9. The field dependence of the inductive critical current density in a $YBa_2Cu_3O_{6.2}Br_{0.9}$ single crystal at different temperatures for fields parallel to the c axis. The solid lines are guides for the eye. The inset shows the corresponding field dependence data for a $YBa_2Cu_3O_{7-y}$ single crystal by Lan, Liu, and Shelton (Ref. 27). The temperatures listed in the inset apply to each curve, consecutively.

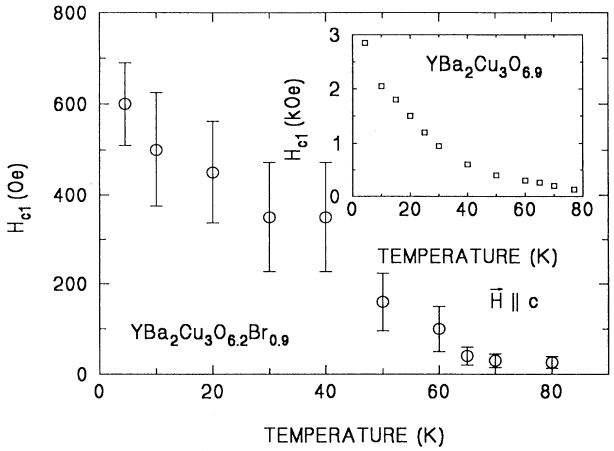

FIG. 11. The temperature dependence of the lower critical field H_{c1} for $H \parallel c$ axis for a $YBa_2Cu_3O_{6.2}Br_{0.9}$ single crystal. The inset shows the corresponding data for a $YBa_2Cu_3O_{7-y}$ single crystal by Lan, Liu, and Shelton (Ref. 12).

with J_c of a fully oxygenated YBCO single crystal shown in the inset of Fig. 9,[27] the J_c values of our brominated YBCO single crystals are noticeably suppressed, especially at higher fields and temperatures. Moreover, J_c for the brominated samples exhibits a much stronger dependence on H than for the fully oxygenated samples. Note that since the resistivity for the brominated YBCO becomes too low to be measured conveniently for the temperature and field range considered in Figs. 9 and 10, the corresponding pinning energies in this range are unavailable for comparison with the J_c values presented here.

Figure 11 plots the measured lower critical field H_{c1} versus temperature of a brominated YBCO single crystal. The inset shows the corresponding result by Lan, Liu, and Shelton[12] on a fully oxygenated YBCO single crystal for H parallel to the c axis. The anomalous upturn of H_{c1} at low temperature ($T < 50$ K) for both the fully oxygenated and the brominated YBCO single crystals can be attributed to the appearance of low-temperature surface barriers.[28] For the high-temperature regime ($T > 50$ K), using the relation derived from the anisotropic GL theory[29]

$$H_{c1} \sim \frac{\Phi_0}{4\pi\lambda_{ab}^2}, \tag{10}$$

where λ_{ab} is the penetration depth for $H \parallel c$ axis and Φ_0 the flux quantum, the value of $(H_{c1}^{\mathrm{YBCO}}/H_{c1}^{\mathrm{YBCO\text{-}Br}})$ between 2 and 3 implies that

$$2 \le \left(\frac{\lambda_{ab}^{\mathrm{YBCO\text{-}Br}}}{\lambda_{ab}^{\mathrm{YBCO}}}\right)^2 \le 3. \tag{11}$$

From the relation $\lambda_{ab}^2 \propto m_{ab}/n_s$ (Ref. 29) with m_{ab} the effective mass in the ab plane and n_s the density of the superconducting electrons which is taken to be equal to the carrier densities n_0 and n_{Br} for the pristine and brominated YBCO samples, respectively, we get

$$\frac{1}{2} \ge \left(\frac{n_{\mathrm{Br}}}{n_0}\right) \ge \frac{1}{3}, \tag{12}$$

assuming m_{ab} is the same. The reduction of the carrier density in Eq. (12) by a factor of 2–3 by bromination is consistent with the observed equivalent decrease in the plasma frequency (from $\sim$10 000 cm^{-1} to $\sim$6 000 cm^{-1}).[11] It is interesting to point out that even though the superconducting carrier density is reduced by more than a factor of 2, the corresponding T_c is unaffected for the brominated single crystals relative to the pristine YBCO samples. This lack of variation in T_c as the carrier density significantly decreases is consistent with the well-known plateau observed in T_c of oxygen-deficient $YBa_2Cu_3O_{7-\delta}$ (Refs. 30 and 31) for

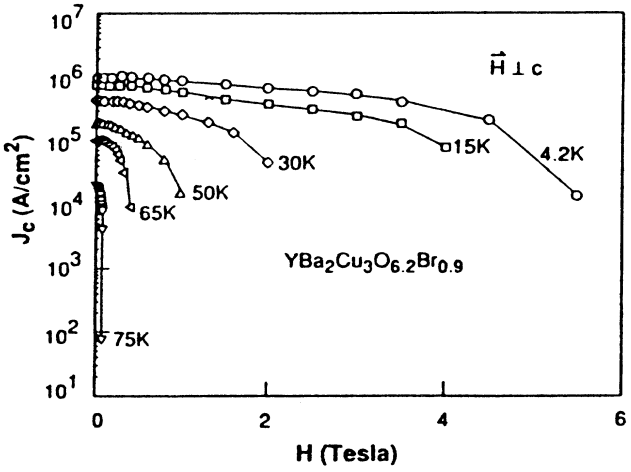

FIG. 10. The field dependence of the inductive critical current density in a $YBa_2Cu_3O_{6.2}Br_{0.9}$ single crystal at different temperatures for fields perpendicular to the c axis. The solid lines are guides for the eye.

$0 \leq \delta \leq 0.12$, where $\delta = 0.12$ corresponds to a decrease in the carrier density by a factor of ~ 2.[32]

VII. SUMMARY

Bromination of deoxygenated YBCO single crystals increases the scattering rate as well as the anisotropy. The relative lack of variation of $\xi_{ab}(0)$ and the reduction of $\xi_c(0)$ by a factor of 3 upon bromination of YBCO suggest that Br never enters the CuO_2 planes. The pinning energy for vortex motion in the *ab* plane decreases after bromination and this decrease can be attributed to the increased anisotropy which is measured independently. For vortex motion along the *c* axis, however, the pinning energy decreases or increases depending on temperature and field. Bromination suppresses J_c and makes it strongly dependent on the applied magnetic field. At high temperature, the reduced lower critical field H_{c1} in the brominated YBCO single crystals indicates a reduction in carrier density (by a factor of between 2 and 3) which is consistent with the observed reduction in the plasma frequency.

ACKNOWLEDGMENTS

The authors wish to thank Robert Andrew of Rome Laboratory, Hanscom AFB for assistance with the SQUID measurements. The work at MIT was supported by Subcontract No. B130530 from Lawrence Livermore National Laboratory, with supplementary support provided by Grant No. AFOSR-90-0123. The work at Lawrence Livermore National Laboratory and University of California, Davis was performed under the auspices of the U.S. Department of Energy under Contract No. W-7405-ENG-48.

[1]Yu. A. Ossipyan, O. V. Zharikov, N. S. Sidorov, V. I. Kulakov, D. N. Mogilyanskii, R. K. Nikoloev, V. Sh. Shekhtman, O. A. Volegova, and I. M. Romanenko, Pis'ma Zh. Eksp. Teor. Fiz. **48**, 225 (1988) [JETP Lett. **48**, 246 (1988)].
[2]Yu. A. Ossipyan, O. V. Zharikov, G. V. Norikov, N. S. Sidorov, V. I. Kulakov, L. V. Sipavina, R. K. Nikoloev, and A. M. Gromov, Pis'ma Zh. Eksp. Teor. Fiz. **49**, 61 (1989) [JETP Lett. **49**, 73 (1989)].
[3]H. B. Radousky, R. S. Glass, P. A. Hahn, M. J. Fluss, R. G. Meisenheimer, B. P. Bonner, C. I. Mertzbacher, E. M. Larson, K. D. McKeegan, J. C. O'Brian, J. L. Peng, R. N. Shelton, and K. F. McCarty, Phys. Rev. B **41**, 11 140 (1990).
[4]A. Tressaud, B. Chevalier, B. Lepine, J. M. Dance, L. Lozano, T. Grannec, T. Etourneau, R. Tournier, A. Sulpice, and P. Lejay, Mod. Phys. Lett. B **2**, 1183 (1988).
[5]E. B. Amitin, N. V. Bausck, S. A. Gromilov, S. G. Kozlova, N. K. Moroz, L. N. Mazalov, V. N. Naumov, P. P. Samoilov, S. A. Slobodjan, M. A. Starikov, V. E. Fedorov, G. I. Frolova, and S. B. Erenburg, Physica C **209**, 407 (1993).
[6]Y. X. Jia, J. Z. Liu, M. D. Lan, P. Klavins, R. N. Shelton, and H. B. Radousky, Phys. Rev. B **45**, 10 609 (1992).
[7]Y. A. Ossipyan and O. V. Zharikov, Physica C **162-164**, 79 (1989).
[8]Y. A. Ossipyan, O. V. Zharikov, G. Y. Logvenov, N. S. Sidorov, V. I. Kulakov, I. M. Shmytko, I. K. Bdikin, and A. M. Gromov, Physica C **165**, 107 (1990).
[9]A. Williams, G. H. Kwei, R. B. Von Dreele, A. C. Larson, I. D. Raistrick, and D. L. Bish, Phys. Rev. B **37**, 7460 (1988).
[10]J. D. Jorgensen, M. A. Beno, D. G. Hinks, L. Soderholm, K. J. Volin, R. L. Hitterman, J. D. Grace, I. K. Schuller, C. U. Segre, K. Zhang, and M. S. Kleefisch, Phys. Rev. B **36**, 3608 (1987).
[11]Y. Wang, A. M. Rao, J. G. Zhang, X. X. Bi, P. C. Eklund, M. S. Dresselhaus, P. P. Nguyen, J. S. Moodera, G. Dresselhaus, H. B. Radousky, R. S. Glass, M. J. Fluss, and J. Z. Liu, Phys. Rev. B **45**, 2523 (1992).
[12]M. D. Lan, J. Z. Liu, and R. N. Shelton, Phys. Rev. B **43**, 12 989 (1991).
[13]F. J. Blunt, A. R. Perry, A. M. Campbell, and R. S. Liu, Physica C **175**, 539 (1991).
[14]Yu. T. Pavlyukhin, A. P. Nemudry, N. G. Khainovsky, and V. V. Boldyrev, Solid State Commun. **72**, 107 (1989).
[15]Yu. A. Ossipyan, O. V. Zharikov, V. L. Matukhin, and V. N. Anashkin, Z. Naturforsch. Teil A **47**, 21 (1992).
[16]C. P. Bean, Phys. Rev. Lett. **8**, 250 (1962).
[17]W. A. Fietz and W. W. Webb, Phys. Rev. **178**, 657 (1969).
[18]T. Penney, S. von Molnar, D. Kaiser, F. Holtzberg, and A. W. Kleinsasser, Phys. Rev. B **38**, 2918 (1988).
[19]T. Ito, H. Takagi, S. Ishibashi, T. Ido, and S. Uchida, Nature **350**, 596 (1991).
[20]N. R. Werthamer, E. Helfand, and P. C. Hohenberg, Phys. Rev. **147**, 295 (1966).
[21]Y. Iye, T. Sakakibara, T. Goto, N. Miura, H. Takeya, and H. Takei, Physica C **153-155**, 26 (1988).
[22]J. S. Moodera, R. Meservey, J. E. Tkaczyk, C. X. Hao, G. A. Gibson, and P. M. Tedrow, Phys. Rev. B **37**, 619 (1988).
[23]M. Tinkham, in *Introduction to Superconductivity* (McGraw-Hill, New York, 1975).
[24]T. T. M. Palstra, B. Batlogg, L. F. Schneemeyer, and J. V. Waszczak, Phys. Rev. B **43**, 3756 (1991).
[25]T. T. M. Palstra, B. Batlogg, R. B. van Dover, L. F. Schneemeyer, and J. V. Waszczak, Phys. Rev. B **41**, 6621 (1990).
[26]S. Chakravarty, B. I. Ivelev, and Y. N. Ovchinnikov, Phys. Rev. Lett. **64**, 3187 (1990).
[27]M. D. Lan, J. Z. Liu, and R. N. Shelton, Phys. Rev. B **44**, 233 (1991).
[28]L. Burlachkov, Y. Yeshurun, M. Konczykowski, and F. Holtzberg, Phys. Rev. B **45**, 8193 (1992).
[29]T. P. Orlando and K. A. Delin, in *Foundations of Applied Superconductivity* (Addison-Wesley, Reading, MA, 1991).
[30]W. E. Farneth, R. K. Bordia, E. M. McCarron III, M. K. Crawford, and R. B. Flippen, Solid State Commun. **66**, 953 (1988).
[31]A. J. Jacobsen, J. M. Newsam, D. C. Johnston, D. P. Goshorn, J. T. Lewandowski, and M. S. Alvarez, Phys. Rev. B **39**, 254 (1989).
[32]J. G. Ossandon, J. R. Thompson, D. K. Christen, B. C. Sales, H. R. Kerchner, J. O. Thomson, Y. R. Sun, K. W. Lay, and J. E. Tkaczyk, Phys. Rev. B **45**, 12 534 (1992).